

# Neighboring group stabilization by $\sigma$ -holes

Richard A. J. O'Hair · Craig M. Williams ·  
Timothy Clark

Received: 3 July 2009 / Accepted: 15 July 2009 / Published online: 15 August 2009  
© Springer-Verlag 2009

**Abstract** We have used density-functional theory to investigate the neighboring-group stabilization of iodine, arsenic, and phosphorus-centered oxyanion moieties in species such as deprotonated 2-iodoxybenzoic acid (IBX) and its analogs. The magnitudes of different stabilizing effects and further candidates for analogous stabilization are analyzed.

**Keywords** Density functional theory ·  $\sigma$ -Hole · IBA · IBS · IBX · 2-iodoxybenzoic

## Introduction

The well-established concept of halogen bonding (for a review, see [1]) has recently been extended to a more general approach that uses the concept of the  $\sigma$ -hole [2].

**Electronic supplementary material** The online version of this article (doi:10.1007/s00894-009-0567-1) contains supplementary material, which is available to authorized users.

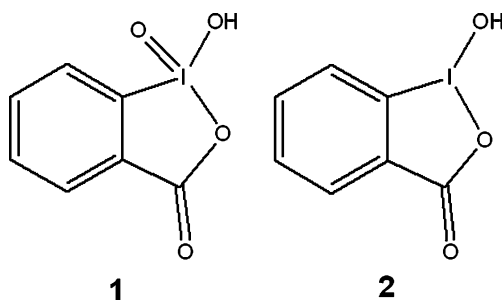
R. A. J. O'Hair  
School of Chemistry and ARC Centre for Free Radical Chemistry  
and Biotechnology, University of Melbourne,  
Melbourne, Victoria 3010, Australia

C. M. Williams  
School of Chemistry and Molecular Biosciences,  
University of Queensland,  
Brisbane 4072 Queensland, Australia

T. Clark (✉)  
Computer-Chemie-Centrum and Interdisciplinary Center  
for Molecular Materials, Friedrich-Alexander-Universität  
Erlangen-Nürnberg,  
Nägelsbachstrasse 25,  
91052 Erlangen, Germany  
e-mail: Tim.Clark@chemie.uni-erlangen.de

Briefly, the  $\sigma$ -hole is an area of positive molecular electrostatic potential collinear with, and opposite, to a bond between an electronegative element in groups 5–7 and of the second long period or higher and an electronegative partner. More recently, the  $\sigma$ -hole concept has been extended to the group 4 elements Si and Ge [3]. The  $\sigma$ -hole results from an electron deficiency in the area of space opposite the covalent bond. It is the result [2] of the *s*-like nature of lone pairs on elements of the higher periods in the periodic table and can be rationalized by hybridization arguments within the linear combination of atomic orbitals (LCAO) approximation.  $\sigma$ -hole bonds can be viewed as a combination of electrostatic and collinear donor-acceptor interactions, much like hydrogen bonds. The  $\sigma$ -hole concept has been demonstrated to be applicable to a surprisingly large number of intermolecular interactions [4–10]. However, as the  $\sigma$ -hole is a general phenomenon, it should also result in intramolecular effects such as neighboring-group stabilization. This result will be most obvious in anions, whose negative centers can be stabilized by interactions with the  $\sigma$ -hole, but intramolecular  $\sigma$ -hole bonding has already been identified for 1,4-intramolecular S...O and Se...O interactions in thiazole and selenazole drugs [8].

Analysis of  $\sigma$ -hole bonding from calculations is difficult because familiar concepts such as the net atomic charge have very little meaning for atoms whose molecular electrostatic potential is very anisotropic [11]. This means that conventional population analyses or schemes to divide the electron density into atomic contributions are not applicable. The donor-acceptor component of  $\sigma$ -hole bonding is related to the established concept of negative hyperconjugation [12, 13] and the anomeric effect [14], but differs in its directionality and in the fact that the  $\sigma$ -hole itself is an observable phenomenon in the isolated mole-



Scheme 1

cule. In the following, we present an energetic and geometrical analysis of intermolecular interactions in which  $\sigma$ -hole bonding plays a role.

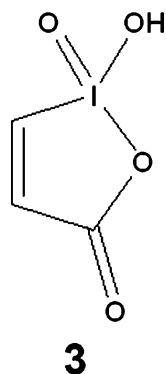
We now present some examples of this type of stabilization and discuss its effect on, for instance proton affinities.

We recently reported  $pK_a$  measurements [15], density-functional theory (DFT) calculations [15, 16], and experimental determinations of the gas-phase proton affinities [16] of the anions of the hypervalent iodine species IBX (2-iodoxybenzoic acid), **1** and IBA (2-iodosobenzoic acid), **2** (Scheme 1).

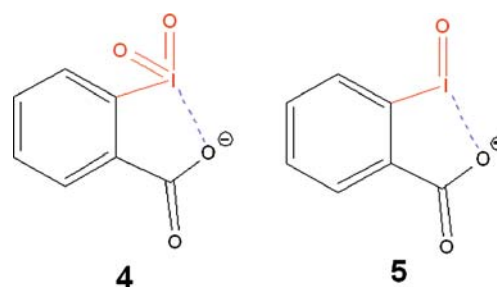
IBX was found to be quite acidic in solution ( $pK_a=6.7$  in water [8]) and its anion to have an experimental proton affinity  $21.5 \text{ kcal mol}^{-1}$  lower than IBA ( $310.7$  vs.  $332.2 \text{ kcal mol}^{-1}$ ) [16]. DFT calculations supported these conclusions. X-ray crystallographic structures [17] of 2-iodyl-4-nitrobenzoate salts reveal the long I-O ring bond shown in the scheme below as a dashed blue line and also revealed by *ab initio* calculations [18] on model compound **3** without the benzo-annellation (Scheme 2).

How do we explain the enhanced acidity of IBX over IBA? In order to analyze this effect, we can regard deprotonated IBX **4** and IBA **5** as benzoates stabilized by a neighboring oxidized iodine center [17, 18] (Scheme 3):

We can use  $\text{PhIO}_2$  and  $\text{PhIO}$  as models for the neighboring iodine acceptor. The molecular electrostatic



Scheme 2



Scheme 3

potential projected onto isodensity surfaces for these two species shows typical areas of positive potential (red) at the backside of the I-O bonds (the  $\sigma$ -hole [2]). One I-O bond in  $\text{PhIO}_2$  has been held coplanar with the phenyl ring to mimic the conformation found in the IBX anion.

## Results and discussion

Figure 1 shows the molecular electrostatic potential calculated at an isodensity surface of  $\text{PhIO}_2$  and  $\text{PhIO}$ . In contrast to other  $\text{XO}_2$  groups [10],  $\text{PhIO}_2$  shows only one  $\sigma$ -hole in the conformation in which one I-O bond is held coplanar to the phenyl ring. The fully optimized ( $C_s$ ) conformation exhibits two smaller and less positive  $\sigma$ -holes

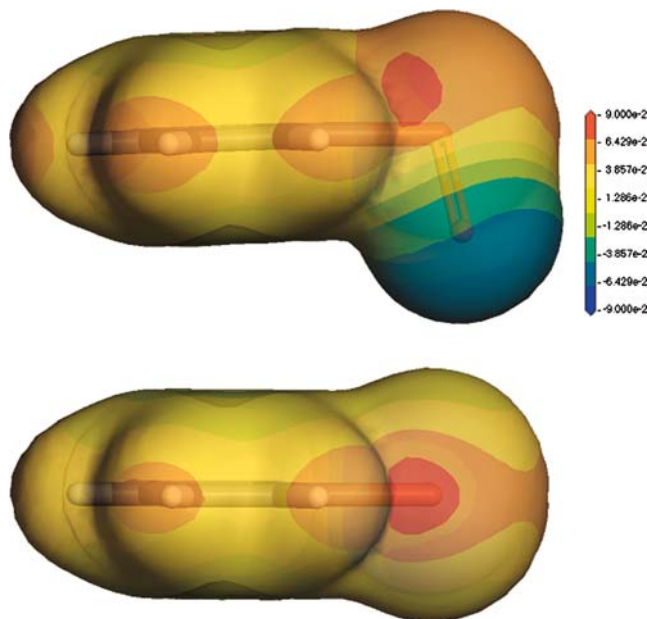


**Fig. 1** Calculated (PW91/dnp) molecular electrostatic potentials projected onto the  $0.017 \text{ e}^- \cdot \text{Bohr}^{-3}$  isodensity surfaces of deprotonated  $\text{PhIO}_2$  (above) and  $\text{PhIO}$  (below). The potential scale is the same in both cases and is given in atomic units. The molecular orientation is chosen to view exactly along the in-plane I-O bond

**Table 1** Total energies (B3LYP/aug-cc-pVTZ, a.u.) and electron affinities (kcal mol<sup>-1</sup>) for PhIO and PhIO<sub>2</sub> and their radical anions. One I-O bond in PhIO<sub>2</sub> and its radical anion has been constrained to lie in the plane of the phenyl ring. The Gaussian archive entries for these calculations are given in the Supporting information

	Total energy		Electron affinity		
	Neutral molecule	Radical anion		Vertical	Relaxed
		Vertical	Relaxed		
PhIO	-602.41621	-677.58277	-602.44319	-8.39	16.92
PhIO <sub>2</sub>	-677.57998	-602.40285	-677.63418	1.75	34.01

collinear with the I-O bonds. We can therefore conclude that the electrostatics around the iodine atom are being influenced strongly by the  $\pi$ -conjugation with the phenyl group. PhIO shows the expected  $\sigma$ -hole collinear with the I-O bond. The  $\sigma$ -hole in PhIO is surprisingly slightly larger than that in PhIO<sub>2</sub>. The most positive potential on the isodensity surface is found in the  $\sigma$ -hole for both molecules and is significantly more positive (+52.5 kcal mol<sup>-1</sup>) for PhIO than for PhIO<sub>2</sub> (+48.5 kcal mol<sup>-1</sup>). The enhanced stability of the IBX anion compared with that of IBA is therefore not a pure electrostatic effect.

However, the intramolecular halogen bonds denoted by blue dashed lines in **4** and **5** also have an electron donor-acceptor (Lewis base-Lewis acid) component. As the electronic nature of the carboxylate anion moiety should be approximately the same for the two systems, the

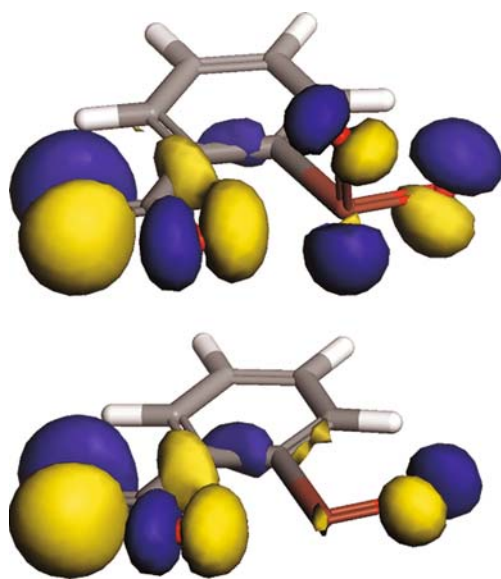
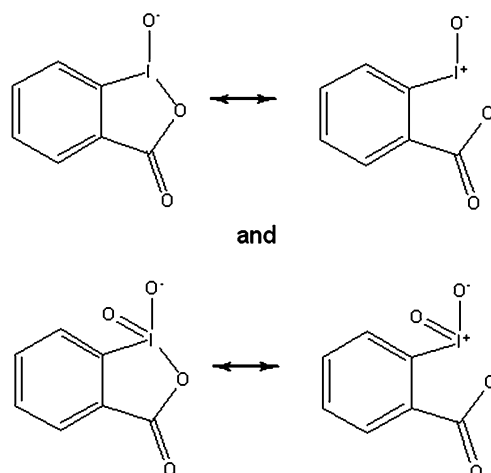


**Fig. 2** The HOMO of deprotonated IBX (above) and the HOMO-1 of deprotonated IBA (below)



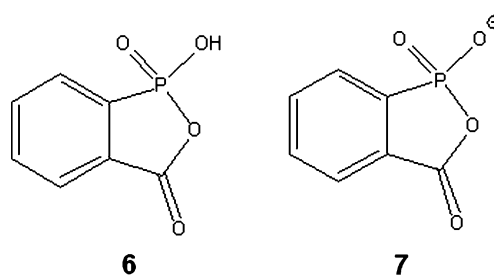
**Scheme 4**

difference must lie in the acceptor properties of the iodine group.

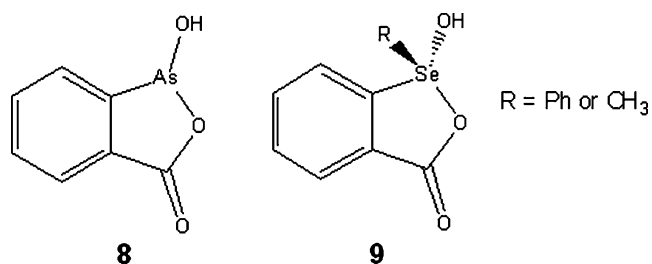
The strength of the substituted iodine moiety can best be judged by calculating the electron affinities of the model compounds PhIO and PhIO<sub>2</sub>. Table 1 shows the B3LYP/aug-cc-pVTZ [19–25] calculated Born-Oppenheimer total energies and electron affinities for fully optimized PhIO and PhIO<sup>-</sup> and for PhIO<sub>2</sub> and its radical anion with one I-O bond constrained to lie in the plane of the phenyl group.

The relaxed electron affinities are of little relevance because PhIO<sup>-</sup> dissociates into a phenyl radical and IO<sup>-</sup> on one-electron reduction and PhIO<sub>2</sub><sup>-</sup> gives a T-shaped radical anion with long I-O bond lengths (see Supporting information). The vertical electron affinities, however, show clearly that PhIO<sub>2</sub> is a significantly better (by 10 kcal mol<sup>-1</sup>) electron acceptor than PhIO.

The highest occupied molecular orbital (HOMO) of deprotonated IBX and the HOMO-1 of IBA demonstrate the donor-acceptor interaction between an in-plane carboxylate lone pair and the opposing  $\sigma^*_{IO}$  antibonding orbital between iodine and oxygen. Figure 2 shows these two orbitals.



**Scheme 5**



Scheme 6

In both cases, the in-plane lone pair of the carboxylate interacts with a  $\sigma^*_{IO}$  orbitals, as we would expect in  $\sigma$ -hole bonding [1, 3]. However, the second oxygen in deprotonated IBX also contributes significantly to stabilizing the  $\sigma^*_{IO}$  orbital, thus making it a stronger acceptor than in deprotonated IBA. Thus, the relative acidities of IBX and IBA can be explained by intramolecular halogen bonding between the incipient carboxylate anion and the  $IO_n$  moiety. In this particular case, the electrostatic effect of the  $\sigma$ -hole should be larger for IO than for  $IO_2$ , but the latter is a better electron acceptor, so that the donor-acceptor component of halogen bonding dominates and makes IBX a stronger acid than IBA. The lengthening of the I-O bonds *anti* to the carboxylate (from 1.862 in  $PhIO_2$  to 1.884 Å in deprotonated IBX and from 1.907 in  $PhIO$  to 1.931 Å in deprotonated IBA, all values calculated at the B3LYP/aug-cc-pVTZ level) underline the importance of electron donation from the carboxylate into the  $\sigma^*_{IO}$  orbital. The fact that the perpendicular IO bond in deprotonated IBX is only marginally lengthened (to 1.864 Å from 1.856 Å) emphasizes the directionality of the interaction.

In valence-bond terms, this stabilization can be expressed by the no-bond resonance structures shown in Scheme 4 [17, 18].

In this case, the  $I=O$  double bond is simply used to denote a “normal” hypervalent iodine-oxygen bond and  $I^+-O^-$  denotes a more highly polarized iodine-oxygen bond

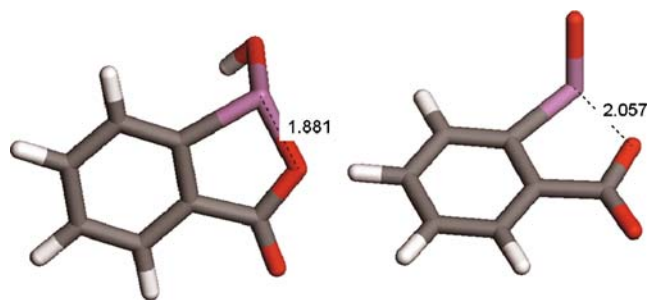


**Fig. 3** The B3LYP/ aug-cc-pVTZ optimized structures of acid 8 (left) and its anion (right)

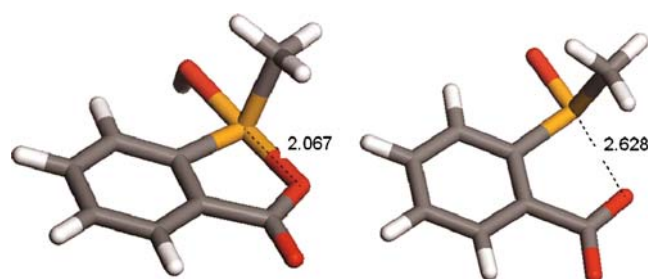


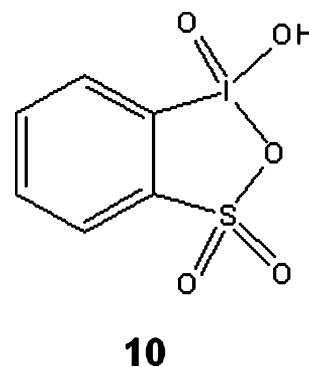
**Fig. 4** The B3LYP/ aug-cc-pVTZ optimized structures of acid 9 (left) and its anion (right)

than normal. We will not consider the question of whether “*d*-orbitals are involved” as it has no meaning outside the (LCAO) approximation and our results can be rationalized using purely *s,p*-hybridization arguments and the existence of relatively low-lying A-O antibonding orbitals [2]. This does not mean that we cannot discuss the form and character of MOs; only the partitioning into AO-contributions is restricted to the LCAO approximation.

#### Other anions stabilized by $\sigma$ -holes on neighboring groups

The prerequisites for neighboring group stabilization of the type discussed above are:

1. A potentially good leaving group (in the above case carboxylate) bound to the  $\sigma$ -accepting center
2. Possibly strain (in the above cases in the five-membered ring) to promote dissociation of the leaving group
3. At least one electronegative substituent (X) on the heavy atom (Y) of the neighboring group to provide a  $\sigma$ -hole
4. A relatively weak X-Y bond to provide a low-lying  $\sigma^*_{XY}$  acceptor orbital



Scheme 7

As a direct analog of IBX, the phosphonic acid **6** might be a candidate for enhanced acidity. However, its anion **7** shows some geometrical evidence of partial dissociation of the ring P-O bond on deprotonation (1.831 Å in the anion, 1.703 Å in the acid), but the effect is not strong. In this case, the strength of the P-O bond renders the  $\sigma^*_{\text{PO}}$  orbital a relatively poor acceptor. The relatively short P-O bond also introduces less strain into the five-membered ring than an I-O bond (Scheme 5).

Obviously, heavier group 5 elements are better candidates for the neighboring group stabilization of the anions, but the corresponding compounds are not isolable. A literature search for compounds that contain the IBX/IBA-like a hydroxyl-substituted heteroatom bound to the oxygen in the five-membered ring suggested that derivatives of the arsenic and selenium compounds **8** [26–28] and **9** [29–32] may be candidates for the type of enhanced acidity described above (Scheme 6).

Calculations on **8** and its anion show the expected geometrical effect, but it is no stronger than that for the phosphonic acid **6**. The ring As-O bond length in **8** is calculated to be 1.881 Å, compared with 2.057 Å for the anion. The optimized geometries are shown in Fig. 3 and given in the Supporting information.

The selenium compound **9** would not normally be expected to be strongly acidic. However, B3LYP/ aug-cc-pVTZ geometry optimizations show a large increase in the ring O-Se bond length; from 2.067 Å in the acid **9** to 2.628 Å in the anion. The optimized geometries are shown in Fig. 4,

Another alternative is the reported sulfonic analog of IBX, IBS **10** [33], in which the potential carboxylate anion is replaced by a sulfonate (Scheme 7).

The optimized structures of **10** and its anion show a strong geometrical effect of deprotonation. The ring O-I bond lengthens for 2.158 Å in the acid to 2.605 Å in the anion. The optimized geometries are shown in Fig. 5 and are given in the Supporting information.

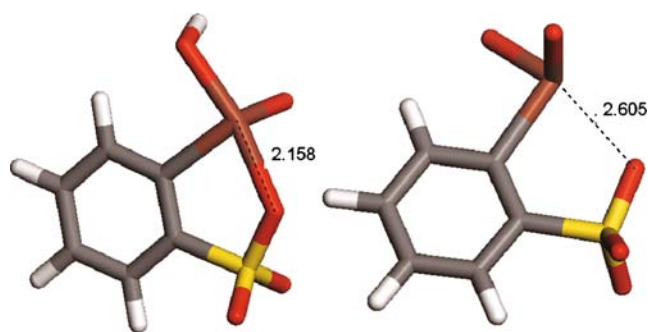
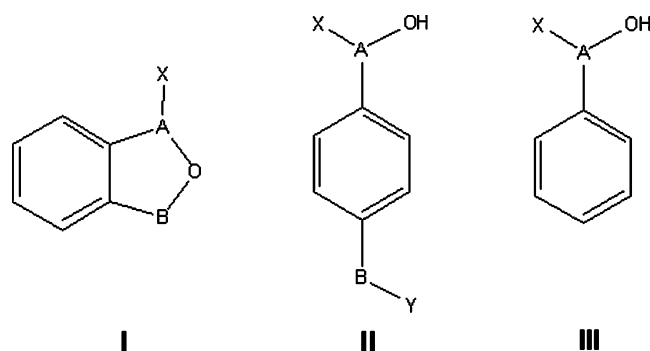


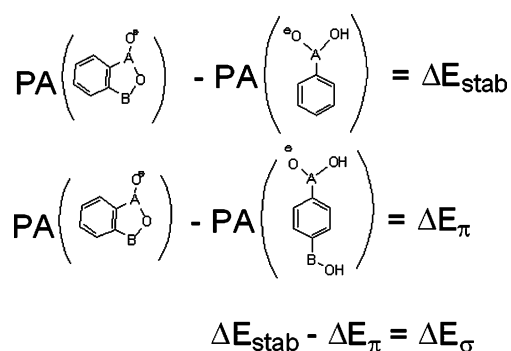
**Fig. 5** The B3LYP/ aug-cc-pVTZ optimized structures of acid **10** (left) and its anion (right)



**Scheme 8**

### Proton affinities

In order to analyze the stabilization of the anions, we introduce the three structures **I–III**, that represent **1**, **2**, **6**, **8**, **9** and **11**, their anions and model compounds, and their deprotonated forms. The unsubstituted acid **III** serves as the standard for the inherent proton affinity of the acid group AX (X is usually OH). The anion of the IBX-analog **I** is stabilized by two main effects; the  $\sigma$ -hole neighboring group effect discussed above and the additional inductive or conjugative stabilization provided by the second substituent B on the aromatic ring. In order to estimate the magnitude of this second effect, we have used the *para*-substituted analog **II**, for which the stabilization by the *para*-substituent must be similar to that given by the *ortho*-equivalent in **I**. Model compound **III** also allows us to assess the energy difference between the oxyanion formed by deprotonation of A and the alternative anion that can be obtained by deprotonating the BY substituent if Y = OH. These model compounds have been designed to allow us to eliminate well-known and common electronic effects such as the inherent proton affinity of the AX(OH) group (*e.g.*, the equivalent of “COOH is more acidic than CH<sub>2</sub>OH”) and the substituent effect of this group on the aromatic system in the AX(OH)-C<sub>6</sub>H<sub>4</sub>-BY system (Scheme 8).



**Scheme 9**



**Table 2** Calculated (B3LYP/aug-cc-pVTZ) stabilization energies (kcal mol<sup>-1</sup>) as defined in the scheme above. The relevant total and zero-point vibrational energies are shown in Table S1 of the Supporting information

A	B	X	II			I		
			Proton affinity	Proton affinity	$\Delta E_{\pi}$	Proton affinity	$\Delta E_{\text{stab}}$	$\Delta E_{\sigma}$
PO <sub>2</sub> <sup>-</sup>	C = O	OH	-327.1	-320.3	-6.8	-315.2	-11.9	-5.0
P = O(OH)	C = O	O <sup>-</sup>		-329.4 (9.1)				
AsO <sup>-</sup>	C = O	OH	-346.3	-340.8	-5.5	-335.3	-11.0	-5.5
AsOH	C = O	O <sup>-</sup>		-332.9 (-7.9)				
Se(CH <sub>3</sub> )O <sup>-</sup>	C = O	OH	-354.0	-347.8	-6.2	-344.4	-9.6	-3.4
Se(CH <sub>3</sub> )OH	C = O	O <sup>-</sup>		-334.1 (-13.7)				
IO <sub>2</sub> <sup>-</sup>	C = O	OH	-339.6	-337.8	-1.8	-319.3	-20.3	-18.5
I = O(OH)	C = O	O <sup>-</sup>		-326.2 (-11.0)				
IO <sup>-</sup>	C = O	OH	-356.9	-347.9	-9.0	-333.0	-23.9	-14.9
I(OH)	C = O	O <sup>-</sup>		-331.5 (-16.3)				
IO <sub>2</sub> <sup>-</sup>	SO <sub>2</sub>	OH	-339.6	-333.8	-5.9	-306.3	-33.4	-27.5
I = O(OH)	SO <sub>2</sub>	O <sup>-</sup>		-319.1 (-14.6)				

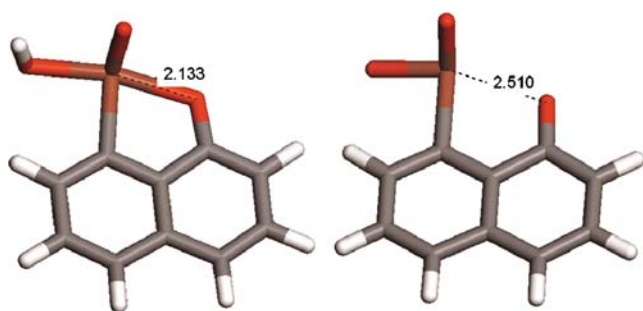
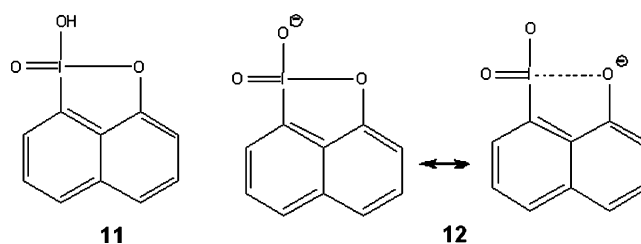
The individual stabilization energies have been estimated using the following scheme (Scheme 9):

$\Delta E_{\text{stab}}$  represents the total stabilization of the oxyanion of the bicyclic IBX analog,  $\Delta E_{\pi}$  due to the *para*-carboxylic acid substituent and  $\Delta E_{\sigma}$  due to the intramolecular bond A-O bond. This intramolecular bond is a combination of the purely electrostatic and donor-acceptor components of the  $\sigma$ -hole interaction and the residual covalent A-O bond minus the additional strain introduced by partially closing the five-membered ring. Table 2 shows that this contribution is relatively small (from 3–5 kcal mol<sup>-1</sup>) for the phosphorus, arsenic and selenium anions, but significantly larger for the iodine ones. The carboxylate group provides less stabilization (15 and 19 kcal mol<sup>-1</sup> in deprotonated IBA and IBX, respectively) than the sulfonate in the IBS anion (28 kcal mol<sup>-1</sup>).

It is not possible to separate the three stabilizing effects outlined above uniquely and is not necessary in the context of this study.

### An alternative ring system

If we retain iodine as the central atom of the neighboring group, we can consider alternatives to the IBX-like bicyclo [4.3.0] ring structure using, for instance, phenolate anions as the neighboring potentially acidic group. One possibility is the naphthoate anion **12** obtained from the acid **11**. In this case, B3LYP/aug-cc-pVTZ calculations show the IO ring bond length in **12** to be 2.531 Å compared with 2.196 Å in **11**. The B3LYP/cc-pDVZ optimized structures of **10** and **11** are shown in Fig. 6 and given in the Supporting information (Scheme 10).

**Fig. 6** The B3LYP/ aug-cc-pVTZ optimized structures of acid **11** (left) and its anion **12** (right)**Scheme 10**

**Acknowledgments** This work was supported by the Deutsche Forschungsgemeinschaft as part of SFB583 “Redox-Active Metal Complexes: Control of Reactivity *via* Molecular Architecture”. The University of Queensland is gratefully acknowledged for financial support.

## References

1. Politzer P, Lane P, Concha MV, Ma Y, Murray JS (2007) *J Mol Model* 13:305–311
2. Clark T, Hennemann M, Murray JS, Politzer P (2007) *J Mol Model* 13:291–296
3. Murray JS, Lane P, Politzer P (2009) *J Mol Model* 15:723–729
4. Murray JS, Lane P, Politzer P (2007) *Int J Quant Chem* 107:2286–2292
5. Politzer P, Murray JS, Lane P (2007) *Int J Quant Chem* 107:3046–3052
6. Murray JS, Lane P, Clark T, Politzer P (2007) *J Mol Model* 13:1033–1038
7. Politzer P, Murray JS, Concha MC (2007) *J Mol Model* 13:643–650
8. Murray JS, Lane P, Politzer P (2008) *Int J Quant Chem* 108:2770–2781
9. Riley KE, Murray JS, Politzer P, Concha MC, Hobza P (2009) *J Chem Theor Comp* 5:155–163
10. Clark T, Murray JS, Lane P, Politzer P (2008) *J Mol Model* 14:689–697
11. Politzer P, Murray JS, Concha M (2008) *J Mol Model* 14:659–665
12. Hoffmann R, Radom L, Pople JA, Schleyer PvR, Hehre WJ, Salem L (1972) *J Am Chem Soc* 94:6221–6223
13. Radom L, Hehre WJ, Pople JA (1972) *J Am Chem Soc* 94:2371–2381
14. Kirby AG (1983) *The anomeric effect and related stereoelectronic effects of oxygen*. Springer, Berlin
15. Gallen MJ, Goumont R, Clark T, Terrier F, Williams CM (2006) *Angew Chem* 118:2995–3000 *Angew Chem Int Ed Engl* 45:2929–2934
16. Waters T, Boulton J, Clark T, Gallen MJ, Williams CM, O’Hair RAJ (2008) *Org Biomol Chem* 6:2530–2533
17. Katritzky AR, Savage GP, Palenik GJ, Qian K, Zhang Z, Durst HD (1990) *J Chem Soc Perkin Trans II* 1657–1661
18. Moss RA, Wilk B, Krogh-Jespersen K, Blair JT, Westbrook JD (1989) *J Am Chem Soc* 111:250–258
19. Frisch MJ, Trucks GW, Schlegel HB, Scuseria GE, Robb MA, Cheeseman JR, Montgomery JA Jr, Vreven T, Kudin KN, Burant JC, Millam JM, Iyengar SS, Tomasi J, Barone V, Mennucci B, Cossi M, Scalmani G, Rega N, Petersson GA, Nakatsuji H, Hada M, Ehara M, Toyota K, Fukuda R, Hasegawa J, Ishida M, Nakajima T, Honda Y, Kitao O, Nakai H, Klene M, Li X, Knox JE, Hratchian HP, Cross JB, Bakken V, Adamo C, Jaramillo J, Gomperts R, Stratmann RE, Yazyev O, Austin AJ, Cammi R, Pomelli C, Ochterski JW, Ayala PY, Morokuma K, Voth GA, Salvador P, Dannenberg JJ, Zakrzewski VG, Dapprich S, Daniels AD, Strain MC, Farkas O, Malick DK, Rabuck AD, Raghavachari K, Foresman JB, Ortiz JV, Cui Q, Baboul AG, Clifford S, Cioslowski J, Stefanov BB, Liu G, Liashenko A, Piskorz P, Komaromi I, Martin RL, Fox DJ, Keith T, Al-Laham MA, Peng CY, Nanayakkara A, Challacombe M, Gill PMW, Johnson B, Chen W, Wong MW, Gonzalez C, Pople JA (2004) *All Calculations used Gaussian 03*. Gaussian, Inc. Wallingford, CT
20. Becke AD (1989) In: Salahub DR, Zerner MC (eds) *The Challenge of d- and f-electrons: Theory and Computation*. American Chemical Society, Washington, DC, chap 12, pp 165–179
21. Vosko SH, Wilk L, Nusair M (1989) *Can J Phys* 58:1200–1211
22. Lee C, Yang W, Parr RG (1988) *Phys Rev B* 37:785–789
23. Becke AD (1993) *J Chem Phys* 98:5648–5652
24. Woon DE, Dunning TH Jr (1993) *J Chem Phys* 98:1358–1371
25. Peterson KA, Figgen D, Goll E, Stoll H, Dolg M (2003) *J Chem Phys* 119:11113–11123
26. Parmar SS, Basra TS, Malhotra RM, Sandhu SS (1980) *Ind J Chem* 19A:886–888
27. Parmar SS, Saluja HK, Bathla HK (1988) *Ind J Chem* 27A:606–608
28. Hundal MS, Hundal G, Parmar SS (1996) *Acta Cryst C* 52:2726–2728
29. Nakanishi W, Ikeda Y, Iwamura H (1982) *J Org Chem* 47:2275–2278
30. Nakanishi W, Matsumoto S, Ikeda Y, Sugawara T, Kawada Y, Iwamura H (1981) *Chem Lett* 1353–1356
31. Dahlen B (1973) *Acta Cryst B* 29:595–602
32. Nakanishi W, Murata S, Ikeda Y, Sugawara T, Kawada Y, Iwamura H (1981) *Tetrahedron Lett* 22:4241–4244
33. Uyanik M, Akakura M, Ishihara K (2008) *J Am Chem Soc* 131:251–262